

Modelling the Astronomical Silicate Features: I. On the Spectrum Subtraction Method

Aigen Li^{1,2,3,*}, J. Mayo Greenberg⁴, and Gang Zhao³

¹ *Theoretical Astrophysics Program, University of Arizona, Tucson, AZ 85719, USA*

² *Princeton University Observatory, Peyton Hall, Princeton, NJ 08544, USA*

³ *National Astronomical Observatories, Chinese Academy of Sciences, Beijing 100012, P.R. China*

⁴ *Raymond and Beverly Sackler Laboratory for Astrophysics, University of Leiden, Postbus 9504, 2300 RA Leiden, The Netherlands*

ABSTRACT

The *assumption of additive absorptivity* by different components in compound particles is a widely used method applied in the literature to the analysis of the chemical and structural properties of astronomical (circumstellar, interstellar, protostellar, and cometary) silicates as well as other materials. The errors intrinsic in this additivity assumption, which, in application to astronomical spectra, amounts in some case to *spectrum subtraction* have not always been adequately considered in previous works on silicate mineralogy. The failings in the “*spectrum subtraction method*” (intrinsically the same as the additive absorptivity assumption) are discussed here in terms of silicate core-ice mantle grains with various shapes. It is shown that these assumptions result in substantial errors for spherical grains. For spheroidal grains, the errors are less significant and the spectrum subtraction method can be used to remove the ice mantle effects. It is demonstrated that there is no significant improvement by considering a distribution of spheroidal shapes. It is further shown that the presence of additional organic mantles substantially modifies the silicate mineralogy interpretation.

Key words: ISM: dust, extinction – infrared: ISM: lines and bands – scattering

1 INTRODUCTION

Silicate grains are ubiquitously present in various cosmic environments. Theoretical efforts have been continuously made to identify the detailed chemical and structural properties of astronomical silicates (Draine & Lee 1984; Ossenkopf, Henning, & Mathis 1992; Greenberg & Li 1996; Mathis 1998; Demyk et al. 1999). On the other hand, during the last decade there has been considerable progress in laboratory measurements of astronomical silicate analogues (see Dorschner 1999 for a review). More recently, the high quality spectroscopic observations in the 10, 18 μ m (as well as the longer wavelength range) silicate bands region of a wide range astronomical objects by the *Infrared Space Observatory* (ISO) together with the rich laboratory data set offer us an unprecedented opportunity to study silicate dust mineralogy.

The analysis of astronomical silicate composition is commonly based on the direct comparison of astronomical absorption/emission features with laboratory data of terrestrial silicate candidates or with theoretical spectra calculated from the optical constants measured for silicate analogues. However, in most regions silicates are combined with other materials. For example, Greenberg (1978) proposed that in the diffuse interstellar medium silicates are coated by a layer of carbonaceous organic refractory; whereas Mathis & Whiffen (1989) suggest that interstellar silicates are combined together with amorphous carbon grains to form porous composite aggregates. GEMS (silicate glass with embedded metal and sulfides) in interplanetary dust particles (IDP) which provide a spectral match to the interstellar 10 μ m Si-O stretching band is usually mantled with or embedded in amorphous carbonaceous material (Bradley et al. 1999). Cometary dust particles are also believed to be a mixture of various forms of silicate and organic (“CHON” particles) materials (Greenberg 1982; Kissel et al. 1986; Wooden

* e-mail: agli@lpl.arizona.edu

et al. 1999). In dense molecular clouds or protostellar disks, the consensus view is that refractory grains are further coated by an outer ice mantle.

In studying silicate composition, it is thus critical to accurately remove the effects caused by the grain’s heterogeneous nature. A simple and commonly adopted method is to simply *subtract* the non-silicate contributions (determined from their characteristic absorption/emission properties) from the entire observational spectrum and then make a comparison between the residual spectrum either directly with laboratory data or with a theoretically derived absorption spectrum by particles using the laboratory optical constants. Hereafter we term this the “*spectrum subtraction*” method.

For example, in a detailed effort to infer the precise composition of the silicate dust around two massive protostellar objects RAFGL 7009S and IRAS 19110+1045, Demyk et al. (1999) subtracted the ice absorption from the total observed absorption to obtain what they presumed to be the observed silicate absorption spectrum as if it could be obtained by adding “ice” absorptivity to the absorption spectrum for bare spherical silicate material grains. Two key assumptions here, both of which affect the derived absorption, are that the grains are spherical and that the absorption by a core-mantle particle is the same as the absorption by the core plus the absorption by the mantle. We term this the “*absorption additivity assumption*”. Note the spectrum subtraction method and the absorption additivity assumption are intrinsically the same. On the basis of this method, Demyk et al. (1999) then modelled the observed silicate absorption spectrum by performing Mie calculations (together with effective medium theory) of spherical porous grains of various compositions.

In the current studies of the crystallinity of circumstellar silicate grains, the circumstellar dust emission spectra are often modelled as co-added emissivities of individual dust components in spite of the fact that (at least) some dust components are actually not separated (e.g., Malfait et al. 1998). The absorption additivity approach has also been applied to cometary silicate analysis (see e.g. Brucato et al. 1999).

The absorption additivity (spectrum subtraction) method takes as a *premise* that the coupling between the silicate and non-silicate materials is negligible. It is obvious that such a premise is physically incorrect (e.g. see Bohren & Huffman 1983). However, this fundamental question has not always been adequately considered in modelling the silicate emission/absorption features in the literature. An equally important problem has to do with the effect of particle shape on the absorption spectrum.

The purpose of this work is not to model any specific astronomical objects, but to address the question of to what extent or in what circumstances such a premise is valid or acceptable. In doing so we will consider a simple case: silicate grains coated by an ice mantle as frequently proposed in the literature although it is likely that an inner carbonaceous mantle may also be present (Greenberg 1978). In §2 we summarize the optical constants employed in this paper. In §3 we discuss the spectrum subtraction method in terms of spherical shape. §4 is devoted to spheroidal shape. We extend then to a distribution of shapes in §5. In §6 we discuss the implications of a more realistic model; i.e., the coated core-mantle spheroidal grains. We summarize our results in §7. In a subsequent paper we will perform detailed modelling on the interstellar silicate bands and discuss the depletion of heavy elements and its implication on dust models (Zhao, Li, & Greenberg 2001).

2 OPTICAL PROPERTIES OF DUST MATERIALS

We consider three types of dust materials: amorphous silicates, carbonaceous organic refractories, and ices. We take the dielectric functions of amorphous olivine MgFeSiO_4 and organic refractory materials from Li & Greenberg (1997). For ices, we consider a mixture of $\text{H}_2\text{O} : \text{CH}_3\text{OH} : \text{CO}_2 = 1.3 : 1 : 1$ (80-90K) which provides the best interpretation of the ISO spectra of RAFGL 7009S (Dartois et al. 1999). The incorporation of CH_3OH and CO_2 adds substantial ice mantle effects to the silicate features since they have strong absorptions such as the $9.75\mu\text{m}$ C-O stretching mode of CH_3OH , and the $15.2\mu\text{m}$ C-O bending mode of CO_2 . We note that neither the specific choice of silicate optical constants nor the precise constituents of the ice mixtures will affect our conclusion since in the present paper, we are not intending to reproduce any specific observations but rather to demonstrate the effects of grain shape and the presence of an ice mantle and therefore to explore the validity of the spectrum subtraction method. We defer our detailed modelling of astronomical silicates to Zhao et al. (2001) where the chemical variations of silicate, carbonaceous, and ice materials, and grain shapes and morphology (porosities) will be discussed in detail.

Since there are no existing optical constants available for such an $\text{H}_2\text{O} : \text{CH}_3\text{OH} : \text{CO}_2 = 1.3 : 1 : 1$ mixture, we construct a set of synthetic refractive indices from the existing data for pure H_2O at 80K, pure CH_3OH at 75K, pure CO_2 at 70K (Hudgins et al. 1993; with mass densities $\approx 1.00, 1.23, 1.56 \text{ g cm}^{-3}$, respectively) by applying the Bruggeman Effective Medium Theory (EMT) (Bohren & Huffman 1983) and assuming a volume fraction of $\text{H}_2\text{O} : \text{CH}_3\text{OH} : \text{CO}_2 = 1 : 1.1 : 1.2$. Theoretical spectra calculated from the synthetic optical constants are consistent with the laboratory IR spectrum of Ehrenfreund et al. (1999). Again, we emphasize here that the precise knowledge of the optical constants of ices is not critical since the purpose of this paper is not to infer the exact dust composition.

3 SPHERICAL GRAINS

We first consider spherical grains. Under the condition of $x = 2\pi a/\lambda \ll 1$ and $|mx| \ll 1$ (a is the grain radius, m is the grain refractive index which relates to the dielectric function ϵ through $\epsilon = m^2$), the absorption cross section of a core-mantle spherical grain C_{abs} can be calculated from the Rayleigh approximation (van de Hulst 1957)

$$C_{\text{abs}}/V = 3 \frac{2\pi}{\lambda} \text{Im} \left\{ \frac{(\epsilon_m - 1)(\epsilon_c + 2\epsilon_m) + f_c(2\epsilon_m + 1)(\epsilon_c - \epsilon_m)}{(\epsilon_m + 2)(\epsilon_c + 2\epsilon_m) + f_c(2\epsilon_m - 2)(\epsilon_c - \epsilon_m)} \right\} \quad (1)$$

where V is the dust volume; ϵ_c and ϵ_m are the complex dielectric functions for the core and mantle materials, respectively; f_c is the volume fraction of the core. The scattering cross sections C_{sca} are much smaller than C_{abs} so that the extinction cross sections $C_{\text{ext}} \approx C_{\text{abs}}$.

We carried out calculations for spherical silicate core-ice mantle grains, taking the silicate core size $a_{\text{sil}} = 0.07\mu\text{m}$, a typical size for the interstellar silicate dust (Li & Greenberg 1997). Note the knowledge of the exact grain size is not critical since interstellar grains ($\sim 0.1\mu\text{m}$) are in the Rayleigh limit in the wavelength range of interest here and also because of this no size distribution is needed.

In Fig. 1a we plot the absorption cross section of the core-mantle grain $C_{\text{abs}}^{\text{sil+ice}}$ with $a_{\text{sil}}=0.07\mu\text{m}$, $f_{\text{sil}}=2/3$ (the volume fraction of the silicate core, $\equiv 1 - V_{\text{ice}}/V_{\text{sil+ice}}$) in the silicate features region. Also plotted are the absorption cross sections for a pure silicate grain $C_{\text{abs}}^{\text{sil}}$ with the same size as the silicate core, and from a pure ice grain $C_{\text{abs}}^{\text{ice}}$ with size $a_{\text{ice}} \approx 0.0556\mu\text{m}$ corresponding to the volume of the ice mantle. Note that the pure ice grain spectrum closely reproduces the ice features of the core-mantle grain. According to the spectrum subtraction method, the contribution of the silicate core to the total absorption cross section $\approx C_{\text{abs}}^{\text{sil-SSM}} \equiv C_{\text{abs}}^{\text{sil+ice}} - C_{\text{abs}}^{\text{ice}}$. However, as clearly illustrated in Fig. 1a, the $C_{\text{abs}}^{\text{sil-SSM}}$ spectrum deviates significantly from that of the pure silicate grain $C_{\text{abs}}^{\text{sil}}$: the peak position of both the $10\mu\text{m}$ Si-O and the $18\mu\text{m}$ O-Si-O features shift to longer wavelengths; both features have a broader red wing with an error $\chi_{\text{SSM}} \equiv C_{\text{abs}}^{\text{sil-SSM}}/C_{\text{abs}}^{\text{sil}} - 1 \approx 8\%$ for the $10\mu\text{m}$ wing and $\approx 12\%$ for the $18\mu\text{m}$ wing. These differences are comparable to some of the differences ascribed by Demyk et al. (1999) to different materials and/or different porosities (for example, the simple spherical enstatite and olivine fits to the silicate absorption spectra [*with ice absorptions subtracted*] of RAFGL 7009S and IRAS 19110 which were rejected by Demyk et al. fail to reproduce the red wing by $< 10\%$ for $\lambda < 18\mu\text{m}$ and $< 20\%$ for $18 < \lambda < 20\mu\text{m}$). In light of this, Demyk et al. (1999)'s invoking of *an admixture of iron, aluminum and some degree of porosity* to explain the red wing of the $18\mu\text{m}$ feature seems unnecessary since it may be just an artifact of the spectrum subtraction method they adopted (see their §4.2 and Fig. 4).

We have also considered the variation of the ice mantle thickness. For illustration we present in Fig. 1b the errors χ_{SSM} caused by the spectrum subtraction method for $f_{\text{ice}} \equiv V_{\text{ice}}/V_{\text{sil+ice}} = 1/5$ (dotted), $1/3$ (solid), and $1/2$ (dashed), respectively. Fig. 1b shows that the spectrum subtraction method can not give acceptable results even for a very thin layer of ice mantle ($\approx 0.0054\mu\text{m}$ for $f_{\text{ice}} = 1/5$).

4 SPHEROIDAL GRAINS

Cosmic dust grains are unlikely to be spherical. On the contrary, polarization of starlight implies both nonsphericity and alignment. We now consider spheroidal shape which can be exactly solved in the Rayleigh limit. For an ensemble of randomly oriented spheroidal grains[†], the absorption cross section is (Greenberg 1972; Lee & Draine 1985)

$$C_{\text{abs}} = \frac{1}{3}C_{\text{abs}}^{\parallel} + \frac{2}{3}C_{\text{abs}}^{\perp} \quad (2)$$

where $C_{\text{abs}}^{\parallel}$ and C_{abs}^{\perp} are the absorption cross sections for light polarized parallel and perpendicular, respectively, to the grain symmetry axis. In the Rayleigh limit, for *confocal* core-mantle spheroidal grains we can calculate the absorption cross sections $C_{\text{abs}}^{\parallel,\perp}$ from (Gilra 1972; Draine & Lee 1984)

$$C_{\text{abs}}^{\parallel,\perp}/V = \frac{2\pi}{\lambda} \text{Im} \left\{ \frac{(\epsilon_m - 1) \left[L_c^{\parallel,\perp}(\epsilon_c - \epsilon_m) + \epsilon_m \right] + f_c(\epsilon_c - \epsilon_m) \left[L_m^{\parallel,\perp}(1 - \epsilon_m) + \epsilon_m \right]}{\left[L_c^{\parallel,\perp}(\epsilon_c - \epsilon_m) + \epsilon_m \right] \left[1 + L_m^{\parallel,\perp}(\epsilon_m - 1) \right] + f_c L_m^{\parallel,\perp}(1 - L_m^{\parallel,\perp})(\epsilon_c - \epsilon_m)(\epsilon_m - 1)} \right\} \quad (3)$$

[†] Similar results are expected for aligned grains; for example, the deviation $\chi' \equiv \sqrt{\sum \{ [C_{\text{abs}}^{\text{sil+ice}} - C_{\text{abs}}^{\text{ice}}] / C_{\text{abs}}^{\text{sil}} - 1 \}^2 / N}$ for the wavelength range of $8.5 \leq \lambda \leq 20\mu\text{m}$ (N is the number of data points) from 3:1 prolate grains of perfect spinning alignment with $f_{\text{ice}}=1/3$ is about 0.023 in comparison with $\chi' = 0.020$ for randomly oriented prolates.

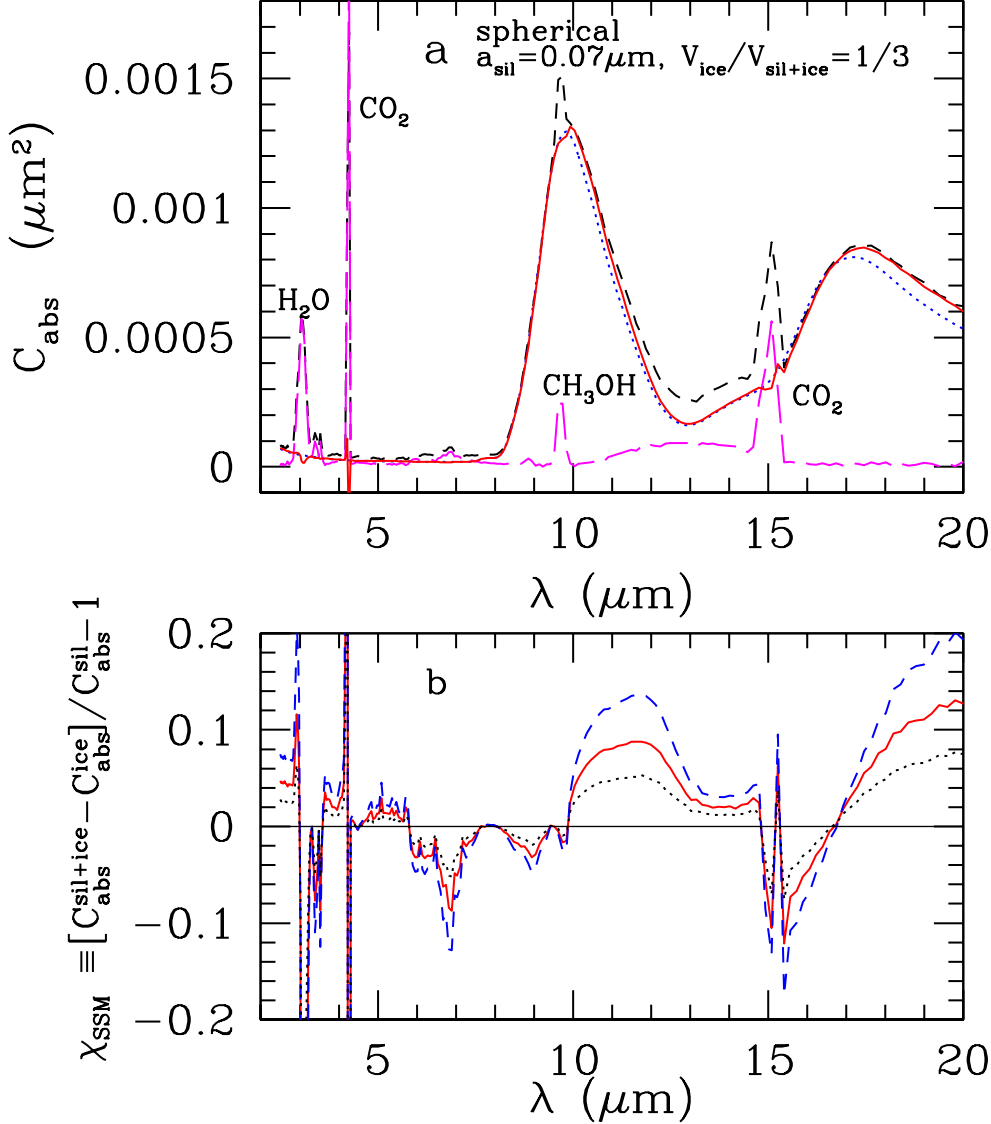


Figure 1. **a:** Absorption cross sections of spherical grains. Dashed ($C_{\text{abs}}^{\text{sil+ice}}$): silicate core-ice mantle grains with a silicate core radius $0.07\mu\text{m}$ and a silicate volume fraction $f_{\text{sil}} = 2/3$ (i.e., $f_{\text{ice}} = 1/3$); long dashed ($C_{\text{abs}}^{\text{ice}}$): the volume-equivalent sphere for the ice mantle; dotted ($C_{\text{abs}}^{\text{sil}}$): a pure silicate sphere with the same size as the silicate core of the core-mantle dust; solid: $C_{\text{abs}}^{\text{sil-SSM}}$. In the framework of the SSM, one should have $C_{\text{abs}}^{\text{sil-SSM}} \approx C_{\text{abs}}^{\text{sil}}$. The contrast between $C_{\text{abs}}^{\text{sil-SSM}}$ (solid) with $C_{\text{abs}}^{\text{sil}}$ (dotted) indicates the unapplicability of the SSM to spherical grains. **b:** The errors χ_{SSM} caused by the spectrum subtraction method for $f_{\text{ice}} = 1/5$ (dotted), $1/3$ (solid), and $1/2$ (dashed). The errors in the red wings of the $10\mu\text{m}$ and $18\mu\text{m}$ features are comparable to the differences ascribed by Demyk et al. (1999) to different materials and/or different porosities (see our text and their §4.2 and Fig. 4). The sharp features at $3.1, 4.2, 9.75,$ and $15.2\mu\text{m}$ are due to the incompleteness in subtracting the ice features. This will not affect our conclusion since in this work we are mainly interested in the broad 10 and $18\mu\text{m}$ silicate bands.

where L_c^{\parallel} , L_c^{\perp} , L_m^{\parallel} , and L_m^{\perp} are the depolarization factors of the core and mantle parallel and perpendicular, respectively, to the grain symmetry axis. The depolarization factors L^{\parallel} , L^{\perp} relate to each other through $L^{\perp} = (1 - L^{\parallel})/2$ because of rotational symmetry and characterize grain shape via Eq.(4):

$$L^{\parallel} = \begin{cases} \frac{1-e^2}{e^2} \left[\frac{1}{2e} \ln \left(\frac{1+e}{1-e} \right) - 1 \right], & \text{for prolate } (a > b) \\ \frac{1+e^2}{e^2} \left(1 - \frac{1}{e} \tan^{-1} e \right), & \text{for oblate } (a < b) \end{cases} \quad (4)$$

where the eccentricity e is given by the two semiaxes a and b (with a semiaxis along the symmetry axis and b semiaxis perpendicular to the symmetry axis)

$$e = \begin{cases} \sqrt{1 - (b/a)^2}, & \text{for prolate } (a > b) \\ \sqrt{(b/a)^2 - 1}, & \text{for oblate } (a < b) \end{cases} \quad (5)$$

and the eccentricities of core and mantle e_c , e_m ($e_c > e_m$) relate to each other through

$$f_c = \begin{cases} \frac{1 - e_c^2}{e_c^3} \frac{e_m^3}{1 - e_m^2}, & \text{for prolate } (a_m > b_m) \\ \frac{1 + e_c^2}{e_c^3} \frac{e_m^3}{1 + e_m^2}, & \text{for oblate } (a_m < b_m) \end{cases} \quad (6)$$

In the special case of $e_c = e_m = e$, Eq.(3) reduces to the solution for a homogeneous spheroidal grain

$$C_{\text{abs}}^{\parallel, \perp} / V = \frac{2\pi}{\lambda} \text{Im} \left\{ \frac{\epsilon - 1}{(\epsilon - 1)L^{\parallel, \perp} + 1} \right\} \quad (7)$$

By applying the method described above, we calculate the absorption cross sections of *confocal* silicate core-ice mantle spheroidal grains with a volume-equivalent sphere radius (the radius of the equivalent sphere having the same volume as the spheroid) $r_{\text{sil}}^{\text{eq}} = (ab^2)^{1/3} = 0.07\mu\text{m}$ for the silicate core and a variable ice mantle controlled by f_{sil} . We first consider $a/b = 3$ prolate core-mantle grains with $r_{\text{sil}}^{\text{eq}} = 0.07\mu\text{m}$ ($a/b = 3$ is for the ice mantle; the corresponding a/b for the silicate core is ≈ 3.57 if $f_{\text{sil}}=2/3$). The reason for choosing an $a/b = 3$ prolate shape is that Greenberg & Li (1996) found that it provides the best fit to the 10, 18 μm silicate polarization features of the Becklin-Neugebauer (BN) object in terms of ice-coated core-mantle dust grains. Also calculated are 1) $C_{\text{abs}}^{\text{ice}}$, the absorption cross section of the volume-equivalent pure ice prolate ($a/b = 3$); 2) $C_{\text{abs}}^{\text{sil}}$, the absorption cross section of the volume-equivalent pure silicate prolate with $a/b \approx 3.57$ determined from Eqs.(5,6); and 3) the ice mantle “subtracted” silicate absorption $C_{\text{abs}}^{\text{sil-SSM}}$. In Fig. 2a we plot the corresponding errors χ_{SSM} for $f_{\text{ice}}=1/5$ (dotted), 1/3 (solid), and 1/2 (dashed).

As can be seen in Fig. 2a, $C_{\text{abs}}^{\text{sil-SSM}}$ is closer to $C_{\text{abs}}^{\text{sil}}$ in comparison with the spherical model (§3). The errors χ_{SSM} for the red wings of the 10 μm and 18 μm features are respectively $\sim 2.5\%$ and $\sim 2\%$ (for $f_{\text{sil}}=2/3$), in sharp contrast to those of the spherical model ($\sim 8\%$ and $\sim 12\%$; see Fig. 1b).

Similarly, we carried out the same calculations but for oblate grains with $a/b = 1/2$ (the core has $a/b \approx 1/2.52$). The $a/b = 1/2$ oblate shape was chosen since it was shown to provide a better match than any other shapes to the 3.1 μm ice polarization feature (Lee & Draine 1985) and the 10 μm silicate polarization feature (Hildebrand & Dragovan 1995) in terms of ice-coated silicate grains (without an intermediate carbonaceous mantle). In Fig. 2b we plot χ_{SSM} for $f_{\text{ice}}=1/5$ (dotted), 1/3 (solid), and 1/2 (dashed) for oblate grains. The results are very similar to the $a/b = 3$ prolate model (Fig. 2a). The errors are $< 3\%$ for the red wings of the 10 μm and 18 μm features.

From these results we conclude that for spheroidal grains, the spectrum subtraction method works better than for spherical grains[‡]. Lacking prior knowledge of the *true* shape of dust grains, the spectrum subtraction method, as a first approximation, can be adopted to study the silicate mineralogy if grains are taken to be spheroidal. This does not necessarily imply that grains need to be spheroidal. What it does imply is that the errors caused by the spectrum subtraction method, in reducing the silicate mineralogy in terms of a spherical shape, are larger than those of spheroidal shapes. If the choice of spheroidal shapes seems rather arbitrary despite the fact that the error χ_{SSM} is indeed smaller, we remind the reader that the spectrum subtraction method is physically incorrect. A better approach to the silicate mineralogy problem is to carry out iterative modelling of the observational spectra using Mie theory together with the effective medium theory or the discrete-dipole approximation for various shapes (e.g. see Zhao et al. 2001).

5 GRAINS WITH A CONTINUOUS DISTRIBUTION OF ELLIPSOIDS (CDE)

The shape of a spheroidal grain is characterized by its eccentricity e (and the depolarization factors L^{\parallel} , L^{\perp} via Eq.[4]). We now extend §4 where only a single shape (a single eccentricity) is considered to an average of a distribution of shapes (for the same volume grain). We assume two kinds of shape distribution functions: 1) $dP/dL^{\parallel} = \text{constant}$, i.e., all shapes are equally probable (Bohren & Huffman 1983); 2) $dP/dL^{\parallel} = 12L^{\parallel}[1 - L^{\parallel}]^2$ (Ossenkopf, Henning, & Mathis 1992; Will & Aannestad 1999) which peaks at spheres ($L^{\parallel} = L^{\perp}=1/3$) and is symmetric about spheres with respect to eccentricity and drops to zero for the extreme cases ($e \rightarrow 1$ [$L^{\parallel} \rightarrow 0$] infinitely thin needles or $e \rightarrow \infty$ [$L^{\parallel} \rightarrow 1$] infinitely flattened pancakes). Averaging over the shape distribution, we have the resultant absorption cross section $C_{\text{abs}} = \int_0^1 dL^{\parallel} dP/dL^{\parallel} C_{\text{abs}}(L^{\parallel})$ where $C_{\text{abs}}(L^{\parallel})$ is the absorption cross section of a particular shape L^{\parallel} (note L^{\parallel} is for the mantle; the core depolarization factor is derived from

[‡] Why the spheroid model works better is not obvious but it may be related to the fact that the spheroidal absorptivity follows the “material” absorptivity (m'') while spherical one does not (Greenberg et al. 1983; van de Bult et al. 1985).

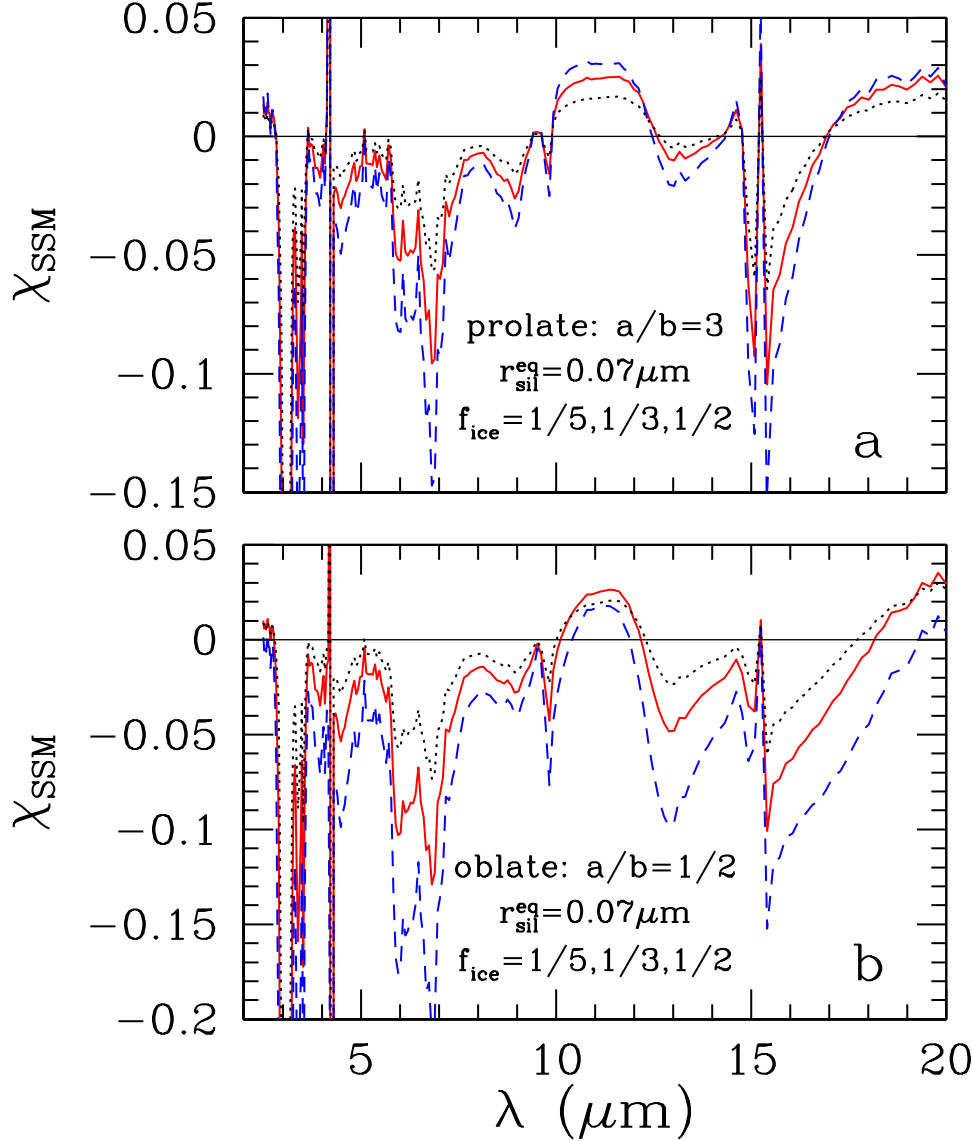


Figure 2. The errors χ_{SSM} caused by the spectrum subtraction method for $f_{\text{ice}}=1/5$ (dotted), $1/3$ (solid), and $1/2$ (dashed) – **a**: for $a/b = 3$ prolate; **b**: for $a/b = 1/2$ oblate. In comparison with the spherical basis, the spectrum subtraction method based on spheroidal grains provides a better approach. The errors at the red wings of the $10\mu\text{m}$ and $18\mu\text{m}$ features are much smaller than those of the spherical model (see Fig. 1b).

Eqs.[4-6]). Again, we assume confocal geometry for core-mantle grains, with the above dP/dL^{\parallel} (as well as e) applying to the outer surface.

We calculated the averaged absorption cross sections of grains with a continuous distribution of ellipsoids (CDE) with $r_{\text{sil}}^{\text{eq}}=0.07\mu\text{m}$, $f_{\text{sil}}=2/3$ for $dP/dL^{\parallel} = \text{constant}$ and $dP/dL^{\parallel} = 12L^{\parallel}[1 - L^{\parallel}]^2$ respectively. We also calculated (1) $C_{\text{abs}}^{\text{sil}}$, the averaged absorption cross sections predicted from the silicate core itself with eccentricities obtained from Eq.(6) for a given set of mantle eccentricities e and f_{sil} ; (2) $C_{\text{abs}}^{\text{ice}}$, the averaged absorption cross sections of ice spheroids with the same volumes and the same eccentricities e as the ice mantles of the core-mantle spheroids; and (3) $C_{\text{abs}}^{\text{sil-SSM}}$.

It is found that the $C_{\text{abs}}^{\text{sil-SSM}}$ of the $dP/dL^{\parallel} = \text{constant}$ model gives similar results to those of the single-shaped spheroidal grains (§4) and leads to smaller errors than the spherical model (see Fig. 3a). In contrast, although the $dP/dL^{\parallel} = 12L^{\parallel}[1 - L^{\parallel}]^2$ model was generally considered as “more physically reasonable” (e.g. see Ossenkopf et al. 1992), it results in a much larger error (even for $f_{\text{ice}} = 1/5$, see Fig. 3b). In particular, $C_{\text{abs}}^{\text{sil-SSM}}$ deviates from $C_{\text{abs}}^{\text{sil}}$ significantly in the peak regions of the $10, 18\mu\text{m}$. This can be understood by the fact that the $dP/dL^{\parallel} = 12L^{\parallel}[1 - L^{\parallel}]^2$ distribution peaks at *spheres* for which the spectrum subtraction method results in a significant error (§3). In comparison with §4, we conclude that the CDE model

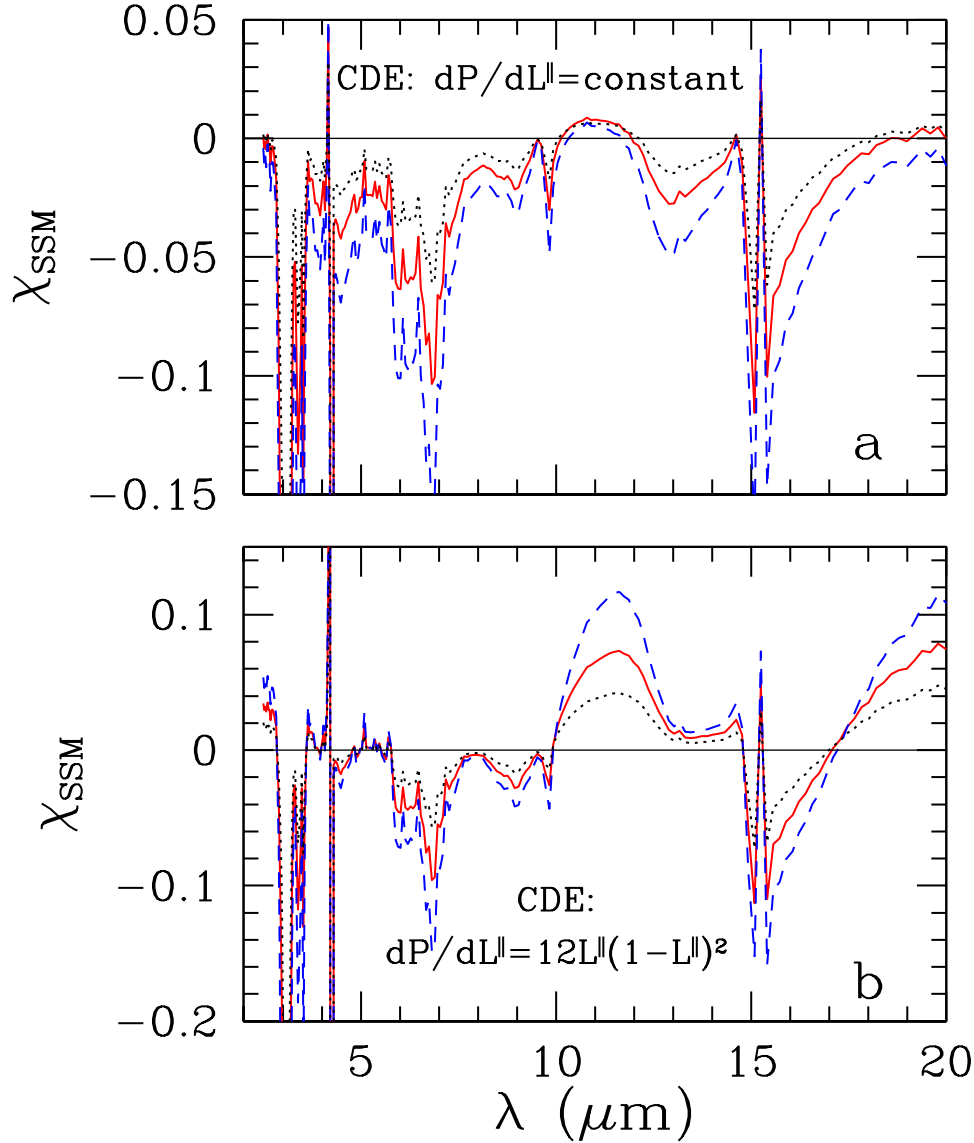


Figure 3. The errors χ_{SSM} caused by the spectrum subtraction method for $f_{\text{ice}}=1/5$ (dotted), $1/3$ (solid), and $1/2$ (dashed) – **a**: for a continuous distribution of spheroids with all shapes equally probable (i.e. $dP/dL^{\parallel}=\text{constant}$); **b**: for a continuous distribution of spheroids with the shape probability distribution $dP/dL^{\parallel} = 12L^{\parallel}(1-L^{\parallel})^2$. The silicate core size is always taken to be $r_{\text{sil}}^{\text{eq}}=0.07\mu\text{m}$.

does not seem to be better suitable to be applied within the framework of the spectrum subtraction method than the single (non-spherical) shape model.

6 COATED CORE-MANTLE GRAINS

Finally, we consider a model in which the silicate core is coated by an carbonaceous mantle (in addition to its outer ice mantle) (Greenberg 1978). We emphasize here the fact that with or without ice mantles there is generally no pure silicate core but rather one which bears an organic mantle as seen in the diffuse interstellar medium, cometary dust, and as implied in molecular clouds (see Greenberg & Li 1999 for a summary). The absorption cross sections for an *equal-eccentricity* three-layered silicate core-carbonaceous inner mantle-ice outer mantle grain is (Farafonov 2001; Voshchinnikov & Mathis 1999)

$$C_{\text{abs}}^{\parallel,\perp}/V = \frac{2\pi}{\lambda} \frac{4\pi}{3} \text{Im} \left\{ \frac{A_2^{\parallel,\perp} - A_1^{\parallel,\perp}}{(A_2^{\parallel,\perp} - A_1^{\parallel,\perp})L^{\parallel,\perp} + A_1^{\parallel,\perp}} \right\} \quad (8)$$

$$\begin{pmatrix} A_1^{\parallel,\perp} \\ A_2^{\parallel,\perp} \end{pmatrix} = \begin{pmatrix} 1 & L^{\parallel,\perp} \\ \epsilon_{\text{om}} & \epsilon_{\text{om}}(L^{\parallel,\perp} - 1) \end{pmatrix} \begin{pmatrix} (\epsilon_{\text{im}}/\epsilon_{\text{om}} - 1)L^{\parallel,\perp} + 1 & (\epsilon_{\text{im}}/\epsilon_{\text{om}} - 1)L^{\parallel,\perp}(L^{\parallel,\perp} - 1)/f_{\text{im}} \\ -(\epsilon_{\text{im}}/\epsilon_{\text{om}} - 1)f_{\text{im}} & -(\epsilon_{\text{im}}/\epsilon_{\text{om}} - 1)(L^{\parallel,\perp} - 1) + 1 \end{pmatrix} \begin{pmatrix} (\epsilon_{\text{c}}/\epsilon_{\text{im}} - 1)L^{\parallel,\perp} + 1 \\ -(\epsilon_{\text{c}}/\epsilon_{\text{im}} - 1)f_{\text{c}} \end{pmatrix} \quad (9)$$

where ϵ_{c} , ϵ_{im} , ϵ_{om} are the dielectric functions for the silicate core, the organic refractory inner mantle, the ice outer mantle, respectively; f_{c} and f_{im} are the volume fractions of the silicate core and the organic refractory inner mantle, respectively. Note that, in contrast to §4, the depolarization factors here are the same for all layers.

We have calculated the absorption cross sections of ice-coated silicate core-organic refractory mantle grains with $r_{\text{sil}}^{\text{eq}}=0.07\mu\text{m}$, $f_{\text{sil}} = f_{\text{or}}=2/5$, $f_{\text{ice}}=1/5$, for $a/b = 3$ prolate as well as for $a/b = 1/2$ oblate, where $f_{\text{sil}} (\equiv f_{\text{c}})$, $f_{\text{or}} (\equiv f_{\text{im}})$, and $f_{\text{ice}} (\equiv 1 - f_{\text{c}} - f_{\text{im}})$ are respectively the fractional volumes of the silicate core, the inner organic refractory mantle, and the outer ice mantle. As not unexpected, $C_{\text{abs}}^{\text{sil-SSM}} (\equiv C_{\text{abs}}^{\text{sil+or+ice}} - C_{\text{abs}}^{\text{ice}})$ is very different from $C_{\text{abs}}^{\text{sil}}$ in the peak positions, the feature widths, and the feature strengths of both the $10\mu\text{m}$ and $18\mu\text{m}$ features. Since the organic refractory material has little absorption around that region, the inclusion of such an inner mantle significantly suppresses the $10\mu\text{m}$ feature (not shown here). It is obvious that silicate grains with carbonaceous coating will not behave like naked silicates. Therefore, it is essential to take into account the possible heterogeneous nature of cosmic dust when modelling the silicate mineralogy.

7 SUMMARY

We have investigated the validity of the “*spectrum subtraction*” method or the “*absorption additivity assumption*” widely adopted in studies of astronomical silicate mineralogy when interpreted using silicate core-ice mantle grains with spherical, spheroidal, and a continuous distribution of ellipsoids (CDE) shapes. We found that: 1) the spectrum subtraction method results in significant errors for spherical grains; 2) for spheroidal grains, the errors are much less significant and the spectrum subtraction method is reasonably successful in removing the ice mantle effects; 3) grains with a uniform distribution of spheroidal shapes produce results little different from those for a single eccentricity; 4) as expected, grains with sphere-peaked distribution of spheroidal shapes, lead to appreciable errors. In addition, we have also discussed the effects caused by the inclusion of an intermediate carbonaceous mantle which is often not taken into account in silicate considerations. As not unexpected, the spectrum subtraction method applied here leads to even more unacceptable errors.

Our conclusion is that, in order to correctly infer the precise composition of astronomical silicates, care should be taken to appropriately take into account the heterogeneous (chemical and/or structural) nature of dust grains. The spectrum subtraction method should be used together with the non-spherical (e.g., prolate or oblate) assumption. It does not appear to have obvious advantages to use a distribution of spheroidal shapes.

ACKNOWLEDGMENTS

A. Li and G. Zhao were deeply saddened by the passing away of Prof. J. Mayo Greenberg (the second author of this paper) on November 29, 2001. As a pioneer in the fields of cosmic dust, comets, astrochemistry, astrobiology and light scattering, Mayo will be remembered forever. It was a great experience for A. Li to work with Mayo in Leiden. We thank Prof. B.T. Draine for his invaluable comments and suggestions; Prof. J.I. Lunine for helpful discussions; Prof. J.S. Mathis for clarification; and Dr. R.H. Lupton for the availability of the SM plotting package. We are grateful to the anonymous referee for helpful advice. We are also grateful to Drs. K. Demyk and L. d’Hendecourt for providing us with their RAFGL 7009S and IRAS 19110 spectra. This research was supported in part by NASA grant NAG5-7030 and NSF grant AST-9619429, and the World Laboratory E-17 Project “Dust and Gas Chemistry in Star-forming Regions”.

REFERENCES

- Bohren, C.F., & Huffman, D.R. 1983, *Absorption and Scattering of Light by Small Particles* (New York: Wiley)
Bradley, J.P., Keller, L.P., Snow, T.P., et al. 1999, *Science*, 285, 1716
Brucato, J.R., Colangeli, L., Mennella, V., Palumbo, P., & Bussoletti, E. 1999, *Planet. Space Sci.*, 47, 773
Dartois, E., Demyk, K., d’Hendecourt, L., & Ehrenfreund, P. 1999, *A&A*, 351, 1066
Demyk, K., Jones, A.P., Dartois, E., Cox, P., & d’Hendecourt, L. 1999, *A&A*, 349, 267
Dorschner, J. 1999, in *Formation and Evolution of Solids in Space*, ed. J.M. Greenberg & A. Li (Dordrecht: Kluwer), 229
Draine, B.T., & Lee, H.M. 1984, *ApJ*, 285, 89
Ehrenfreund, P., Kerkhof, O., Schutte, W.A., et al. 1999, *A&A*, 350, 240
Farafonov, V.G. 2001, *Opt. Spectrosc.*, 90, 574

- Gilra, D.P. 1972, in *The Scientific Results from the OAO-2*, ed. A.D. Code (NASA SP-310), 295
- Greenberg, J.M. 1972, *J. Colloid Interface Sci.*, 39, 513
- Greenberg, J.M. 1978, in *Cosmic Dust*, ed. J.A.M. McDonnell (New York: Wiley), 187
- Greenberg, J.M. 1982, in *Comets*, ed. L.L. Wilkening (Tucson: Univ. Arizona Press), 131
- Greenberg, J.M., van de Bult, C.E.P.M., & Allamandola, L.J. 1983, *J. Phys. Chem.*, 87, 4243
- Greenberg, J.M., & Li, A. 1996, *A&A*, 309, 258
- Greenberg, J.M., & Li, A. 1999, *Adv. Space Res.*, 24, 497
- Hildebrand, R.H., & Dragovan, M. 1995, *ApJ*, 450, 663
- Hudgins, D.M., Sandford, S.A., Allamandola, L.J., & Tielens, A.G.G.M. 1993, *ApJS*, 86, 713
- Kissel, J., Brownlee, D.E., Büchler, K., et al. 1986, *Nature*, 321, 336
- Lee, H.M., & Draine, B.T. 1985, *ApJ*, 290, 211
- Li, A., & Greenberg, J.M. 1997, *A&A*, 323, 566
- Malfait, K., Waelkens, C., Waters, L.B.F.M., et al. 1998, *A&A*, 332, L25
- Mathis, J.S., & Whiffen, G. 1989, *ApJ*, 341, 808
- Mathis, J.S. 1998, *ApJ*, 497, 824
- Ossenkopf, V., Henning, Th., & Mathis, J.S. 1992, *A&A*, 261, 567
- van de Bult, C.E.P.M., Greenberg, J.M., & Whittet, D.C.B. 1985, *MNRAS*, 214, 289
- van de Hulst, H.C. 1957, *Light Scattering by Small Particles* (New York: Wiley)
- Voshchinnikov, N.V. & Mathis, J.S. 1999, *ApJ*, 526, 257
- Will, L.M., & Aannestad, P.A. 1999, *ApJ*, 526, 242
- Wooden, D.H., Harker, D.E., Woodward, C.E., et al. 1999, *ApJ*, 517, 1034
- Zhao, G., Li, A., & Greenberg, J.M. 2001, in preparation